

TITLE

Mixotrophs generate carbon tipping points under warming

SHORT TITLE

Mixotrophs, carbon flux, and warming

AUTHORS

Daniel J. Wieczynski^{1,*} (daniel.wieczynski@duke.edu),

Holly V. Moeller² (holly.moeller@lifesci.ucsb.edu),

Jean P. Gibert¹ (jean.gibert@duke.edu)

AFFILIATIONS

¹Department of Biology, Duke University, Durham NC, 27708, USA

²Department of Ecology, Evolution, and Marine Biology, University of California, Santa Barbara, Santa Barbara, CA 93106, USA

*Corresponding author

KEYWORDS:

Climate Change, Tipping points, Mixotrophy, Alternative stable states, Carbon flux, Ecosystem functioning, Food webs

ARTICLE TYPE: Letter

COUNTS: Words: Abstract (146), Main text (4404); References (67); Figures (4); Tables (1)

STATEMENT OF AUTHORSHIP:

DJW designed the study and performed the mathematical modeling with support from HVM and JPG. DJW wrote the first draft of the manuscript and all authors contributed substantially to revisions.

DATA ACCESSABILITY STATEMENT

All software and data from this study are available on GitHub (upon publication).

ABSTRACT

Mixotrophs are ubiquitous and integral to microbial food webs, but their impacts on the dynamics and functioning of broader ecosystems are largely unresolved. Here, we show that mixotrophy produces a unique, dynamic type of food web module that exhibits unusual ecological dynamics, with surprising consequences for carbon flux under warming. We find that mixotrophs generate alternative stable carbon states across temperatures—including an autotrophy-dominant carbon sink state, a heterotrophy-dominant carbon source state, and cycling between these two. Moreover, warming always shifts this mixotrophic system from a carbon sink state to a carbon source state, but increasing nutrients erases early warning signals of this transition and expands hysteresis. This suggests that mixotrophs can generate critical carbon tipping points under warming that will be more abrupt and less reversible when combined with increased nutrient levels, having widespread implications for ecosystem functioning in the face of rapid global change.

INTRODUCTION

Microbial organisms play a critical role in ecosystem carbon and nutrient cycling (Kayranli *et al.* 2010; Schimel & Schaeffer 2012; Steinberg & Landry 2017; Zhang *et al.* 2018; Geisen *et al.* 2020; Rocca *et al.* 2022) that is likely to change with rapidly shifting global conditions (Zhou *et al.* 2012; Bradford *et al.* 2019; Smith *et al.* 2019; Geisen *et al.* 2021; Wieczynski *et al.* 2021). Understanding the net impacts of global change on ecosystem flux requires untangling the roles of a diverse assortment of ecological strategies within the microbial world (Bengtsson *et al.* 1996; Petchey *et al.* 1999; Gao *et al.* 2019; Thakur & Geisen 2019; Geisen *et al.* 2020; Kuppardt-Kirmse & Chatzinotas 2020).

Mixotrophy is a common strategy within microbial communities, but its impacts on the dynamics of ecosystem processes remains relatively unresolved (Sanders 1991; Jones 2000; Esteban *et al.* 2010; Mitra *et al.* 2014; Jassey *et al.* 2015; Selosse *et al.* 2017; Stoecker *et al.* 2017; Johnson & Moeller 2018; Flynn *et al.* 2019). Mixotrophic organisms use a combination of energy acquisition (or trophic) modes: autotrophy (phototrophy or chemoautotrophy) and heterotrophy (phagotrophy or chemoheterotrophy) (Stoecker 1998; Esteban *et al.* 2010). Although mixotrophy also occurs in plants (Selosse & Roy 2009; Schmidt *et al.* 2013) and animals (Orr 1888; Venn *et al.* 2008; Graham *et al.* 2013), the majority of mixotrophs are microorganisms like bacteria, archaea, protists, and fungi (Selosse *et al.* 2017). Mixotrophic microbes are ubiquitous in terrestrial, freshwater, and marine systems (Sanders 1991; Stoecker 1998; Mieczan 2009; Esteban *et al.* 2010; Worden *et al.* 2015; Selosse *et al.* 2017; Stoecker *et al.* 2017; Flynn *et al.* 2019), and mixotrophy is increasingly recognized as a dominant nutrient acquisition strategy within microbial food webs (Sanders 1991; Mitra *et al.* 2014; Jassey *et al.* 2015; Selosse *et al.*

2017). By acting as both primary producers and consumers, mixotrophs play a unique role in ecosystem carbon and nutrient cycling (Jones 2000; Mitra *et al.* 2014; Jassey *et al.* 2015) that is likely to change with warming (Wilken *et al.* 2013). Elucidating mixotrophic responses to rapidly changing environmental conditions is thus essential for understanding and predicting the impacts of global climate change on ecosystem functioning.

Mixotrophic strategies may be characterized by differential utilization of three basic resources—light, dissolved nutrients, and prey organisms (Jones 1997; Stoecker 1998; Mitra *et al.* 2016). Multiple schemes have been developed to organize mixotrophs according to their dependencies on these core resources (Jones 1997; Stoecker 1998; Mitra *et al.* 2016). Accordingly, mixotrophs generally fall into one of three basic categories: 1) “ideal” mixotrophs equally balance autotrophy and heterotrophy, 2) “phagotrophic algae” are primarily autotrophs that use heterotrophy to supplement either carbon or nutrient needs, and 3) “photosynthetic protozoa” are primarily heterotrophs that supplement carbon needs with autotrophy. However, these strategies are not fixed. Indeed, changes in the availability of light, nutrients, or prey can cause individual organisms to shift from one mode of energy acquisition to another (Stoecker 1998).

Consequently, mixotrophy likely represents a unique type of food web module whose structural and dynamical qualities vary in response to shifts between energy acquisition modes in mixotrophs. Under certain conditions, mixotrophs may benefit more from autotrophy, acquiring carbon primarily via photosynthesis rather than predation (Figure 1, left). Under other conditions, heterotrophy may be favored and carbon acquired primarily via consumption of prey (Figure 1, right). Importantly, mixotrophs may dynamically switch between these energy

acquisition modes as conditions change across space or time. This dynamic blending of energy acquisition modes could introduce novel dynamical behaviors, altering population dynamics, species interactions, and equilibria in ecological communities in ways that are not fully captured by current theoretical frameworks. Although some studies have investigated mixotrophic dynamics using mathematical models (e.g., Thingstad *et al.* 1996; Jost *et al.* 2004; Moeller *et al.* 2016, 2019; Yang *et al.* 2016; Moroz *et al.* 2019), these tend to be tailored to specific systems, organisms, and environmental conditions, potentially missing the full range of dynamical behaviors possible in mixotrophic systems. To begin to explore these possible behaviors—and how they are altered by environmental change—we need a generalizable mixotrophic model that incorporates dynamically shifting energy acquisition modes in response to dynamic changes in the availability of essential resources and variation in environmental conditions. Yet, no single model to date has done this, which precludes us from truly understanding the roles of mixotrophs within food webs and their associated impacts on ecosystem-level functioning.

Additionally, the processes that control mixotrophic population dynamics—autotrophic production (photosynthesis), heterotrophic production (predation), respiration, mortality, etc.—are expected to be accelerated by warming ((Brown *et al.* 2004; Savage *et al.* 2004; Allen *et al.* 2005; Dell *et al.* 2014)), but may exhibit different sensitivities to temperature change. Importantly, autotrophic production exhibits significantly lower sensitivity to increasing temperature than heterotrophic production, as evidenced by temperature sensitivities (in the form of ‘activation energies’) of $\sim 0.32\text{eV}$ and $\sim 0.65\text{eV}$, respectively (Allen *et al.* 2005; López-Urrutia *et al.* 2006; Yvon-Durocher & Allen 2012). Consequently, some empirical (Wilken *et al.* 2013, 2018) and theoretical (Yang *et al.* 2016) evidence suggests that mixotrophs will tend to favor

heterotrophy over autotrophy with warming. But whether this transition will be sudden or gradual, and whether this will be mediated by other environmental change factors (e.g., eutrophication), is virtually unknown.

Here we develop a generalizable mixotrophic food web model to evaluate the impacts of environmental change on mixotrophic dynamics and carbon flux. We address three main questions: 1) Does environmental change (in the form of temperature and nutrient concentration) alter the ecological dynamics and stability of mixotrophic systems?, 2) Does this, in turn, cause shifts in carbon flux states (i.e., carbon sink and carbon source states)?, and 3) Are there early warning signals for tipping points between these states? Our results show that mixotrophic systems undergo complex—but predictable—dynamical transitions between alternative stable carbon states with warming that may be preceded by early warning signals in the form of steady-state cycling behavior. However, these early warning signals disappear and are replaced by an abrupt carbon state shift when warming is accompanied by increasing nutrient levels, which has important implications for ecosystem functioning in a rapidly warming and increasingly anthropogenized world.

MATERIAL AND METHODS

Mixotrophic model

Different types of mixotrophs can be modeled by defining specific dependencies (functional responses) of photosynthesis and consumption on three limiting resources: prey, nutrients, and light (Stoecker 1998). To study the effects of warming, we also incorporate temperature dependence on several rate parameters in our model. We focus our analysis on a model of

mixotrophy representing organisms that are primarily phagotrophic but switch to photosynthesis to obtain carbon when prey are limiting (known as “photosynthetic protozoa”, or Type-III mixotrophs in the terminology of (Stoecker 1998)). Although we study this particular type of mixotroph here, our model can be generalized to any other type of mixotrophs by replacing the functional responses for prey, nutrient, and light dependencies with alternative functional forms.

Our mixotrophic model consists of two ordinary differential equations (ODEs) that define the dynamics of a two species system—a mixotroph (M) and its prey (P):

$$\frac{dM}{dt} = M * (\varphi(T, N_M, P, M) + \varepsilon\lambda(T, P) - \delta_M(T) - m_M(T)) \quad (1a)$$

$$\frac{dP}{dt} = P * \left(\mu_P(T) \frac{N_P}{h_P + N_P} \left(1 - \frac{P}{K_P} \right) - \lambda(T, P) - \delta_P(T) - m_P(T) \right), \quad (1b)$$

where M and P are biomass densities in units of nanograms of carbon per liter (Table 1). The terms φ and $\varepsilon\lambda$ (consumption rate λ multiplied by a conversion efficiency ε) represent the mixotroph’s per-capita biomass production rates from photosynthesis and consumption, respectively:

$$\text{Photosynthesis: } \varphi(T, N_M, P, M) = \mu_M(T) \frac{N_M}{h_M + N_M} e^{-dP^2} \left(1 - \frac{M}{K_M} \right) \quad (2a)$$

$$\text{Consumption: } \varepsilon\lambda(T, P) = \frac{\varepsilon\alpha(T)P}{1 + \alpha(T)P} \quad (2b)$$

Photosynthetic production rate (φ) follows a modified logistic-growth form that incorporates dependencies on temperature (T), nutrient concentration (N_M), prey density (P), and mixotroph density (M). Per-capita photosynthetic production is assumed to decline as mixotroph density approaches a carrying capacity (K_M), due to limitation of essential resources (e.g., light). Nutrient uptake follows Michaelis–Menten kinetics where uptake rate saturates with increasing nutrient concentrations to a maximum rate ($\mu_M(T)$) according to a half-saturation constant (h_M , i.e., the

nutrient concentration at which the foraging rate is half the maximum possible rate). To capture a reduction in photosynthetic investment when prey are abundant, the dependence of photosynthetic production rate on prey density is defined by a logistic decay function (e^{-dP^2}) that declines with increasing prey density at a rate determined by d and saturates at a maximum value as prey density approaches zero (Figure S1a). Consumption rate (λ) follows a type-II functional response that saturates with increasing prey density and has an attack rate of $\alpha(T)$. Biomass loss is accounted for through the parameters δ_M and m_M , which represent respiration and mortality, respectively. The percentage of total production that comes from photosynthesis was calculated as $\phi/(\phi + \varepsilon \lambda) \cdot 100$.

Prey are assumed to be exclusively chemoheterotrophic and also follow a modified logistic form, with dependencies on temperature (T), nutrient concentration (N_P), and prey density (P) defined by Michaelis–Menten kinetics with maximum uptake rate $\mu_P(T)$, a half-saturation constant h_P , and carrying capacity K_P . Prey biomass declines through consumption by the mixotroph (λ), respiration (δ_P), and mortality (m_P).

Temperature dependence

Maximum uptake, attack, mortality, and respiration rates are all assumed to be temperature-dependent (explicitly written as a function of T in Eqns. 1&2) and follow the common Arrhenius form:

$$rate(T) = b_0 e^{-\frac{E_a}{k} \left(\frac{1}{T} - \frac{1}{T_{ref}} \right)} \quad (2)$$

where b_0 is a normalization constant, E_a is activation energy, k is Boltzmann's constant ($8.6 \cdot 10^{-5}$ eV·K⁻¹), and T_{ref} is a reference temperature at which the given rate is equal to b_0 ($T_{ref} = 20^\circ\text{C}$ for all parameters in our model). The temperature sensitivities of each rate are controlled by the activation energies (E_a), which were empirically estimated elsewhere: $E_a = 0.32$ for photosynthetic production (Allen *et al.* 2005) and $E_a = 0.65$ for heterotrophic production and respiration (Brown *et al.* 2004; Dell *et al.* 2011).

Carbon dynamics

To track carbon dynamics, we calculated net CO₂ flux as total system respiration rate minus total system photosynthetic rate:

$$CO_2 \text{ flux} = 3.67 * (\delta_M(T)M + \delta_P(T)P - \varphi(T, n, P, M)M) \quad (4)$$

where $\delta_M(T)M + \delta_P(T)P$ is total system respiration rate and the third term $\varphi(T, n, P, M)M$ represents the rate of carbon uptake for use in photosynthesis. The coefficient 3.67 converts grams of carbon (C) to grams of carbon dioxide (CO₂) ($\text{gCO}_2 / \text{gC} = 44/12 = 3.67$).

Equilibria and stability analysis

We quantified equilibria by numerically solving the system (using Mathematica V13.0.0 (Wolfram Research, Inc. 2021)) across a range of temperatures (19–23°C) and nutrient concentrations (0.45–0.95 ng L⁻¹). The stability and dynamical behavior of equilibria were determined through local stability analysis, i.e., by calculating the eigenvalues (for our system there are two, one for each state variable) of the Jacobian matrix evaluated at equilibrium in each environmental state (i.e., combination of temperature and nutrient concentration), then using those eigenvalues to characterize the stability of equilibria. For eigenvalues with only real parts,

if the dominant (largest) eigenvalue is negative, then the equilibrium is a stable node (non-oscillatory), otherwise, it is an unstable node (non-oscillatory). For complex eigenvalues (with imaginary parts), there were three possible equilibrium behaviors: i) a negative dominant eigenvalue produces a stable focus (damped oscillations), ii) if only one eigenvalue has a positive real part and it is not equal to the conjugate of the other eigenvalue, then this produces an unstable focus (outward spiral), and iii) the existence of all positive real parts when one eigenvalue is equal to the conjugate of the other produces a limit cycle (sustained oscillations). Steady-state dynamics were identified by numerically solving the system for 100,000 time steps and recording the maximum and minimum densities of each species for the last 10,000 time steps. We repeated this process for all equilibria in each environmental state, initializing each simulation with small perturbations from each equilibrium point (equilibrium values + 0.001). This allowed us to calculate long-term stationary dynamics created by limit cycles and degenerate limit cycles.

RESULTS

Effects of temperature on mixotrophic dynamics

Increasing temperature reshapes the dynamical landscape of this mixotrophic system (Figure 2). At low temperatures, a single, stable equilibrium exists where mixotrophs are at an intermediate density and their prey are at very low (or zero) density (Figure 2a, green). At intermediate temperatures, three stable equilibria appear: i) one stable point where both species are at relatively low densities (green), ii) one high-density stable point (red), and iii) a stationary cycle that orbits these two stable points (blue; Figure 2b). At higher temperatures, only one equilibrium exists where both species coexist at relatively high densities (Figure 2c).

239

240 These transitions between stable states are produced by a progression of bifurcations across
241 temperatures (Figure 2d). Multiple equilibria exist across a range of intermediate temperatures
242 (20.06–21.99°C) whose stability and dynamical behavior change as temperature increases. First,
243 a limit cycle appears at 20.06°C (black dashed line), but its stability is disrupted by an unstable
244 node (gray dotted line) separating it from the original stable point (green line), and the long-term
245 dynamics approach the stable point regardless of initial conditions (Figure 2d). Next, at 20.7°C
246 multiple stable states cooccur—one is the original stable point (green) and the other is a
247 stationary cycle (blue lines, gray shading) that orbits the stable point and the unstable limit cycle.
248 The high-density stable point (red) appears at 20.79°C, producing a unique form of tri-stability
249 including all three of the alternative stable states described above (Figure 2b). The stationary
250 cycle disappears at 21.05°C, leaving two alternative, static, stable points, but the low-density
251 stable point (green) quickly becomes a limit cycle that does not sustain cycling at 21.1°C.
252 Instead, the long-term trajectory here always approaches the high-density stable point (red).
253 Eventually, as temperature increases to 22°C, only one, high-density stable point (red) remains
254 (Figure 2c).

255

256 *Effects of temperature on carbon flux*

257 Increasing temperature shifts this mixotrophic system from a net carbon sink (dominated by
258 photosynthesis; Figure 2e), to alternative carbon states (sink and source; Figure 2f), to a net
259 carbon source (dominated by predation; Figure 2g). This sequence of carbon state transitions
260 corresponds with changes in the long-term carbon dynamics of the system due to shifts in the
261 dominant carbon acquisition strategy of the mixotroph. At low temperatures, most of the

mixotroph's biomass production comes from photosynthesis and, after accounting for carbon uptake for use in photosynthesis and carbon release through respiration by both species, the net flux of carbon dioxide (CO₂) in the system is negative (i.e., a net carbon sink) (Figure 2e). At intermediate temperatures, three stable carbon states coexist: i) one carbon-sink state (green), ii) one stationary cycle where production fluctuates between photosynthesis and predation and the system cycles between a carbon-sink state and carbon-source state, respectively (blue), and iii) one carbon-source state where production is dominated by predation and carbon flux is positive (Figure 2f). At high temperatures, predation takes over as the sole form of production and the system becomes a net carbon source (Figure 2g). Because stationary cycles span a range of temperatures separating carbon sink and source states (Figure 2d), this cycling behavior can be considered an early warning signal of this transition.

Combined effects of temperature and nutrient concentration

The temperature-driven progression through alternative stable states is mediated by nutrient concentration (Figure 3). Changes in temperature and nutrient levels leads to a complex equilibrium landscape that produces a rich assortment of behaviors (Figure 3a). Within this landscape, the range of temperatures producing multiple nontrivial equilibria widens with increasing nutrient concentration (Figure 3a; region inside solid black line), creating upper and lower equilibrium planes in three-dimensional space (Figure 3b) consisting of various combinations of stable points and limit cycles that are separated by an interior plane of unstable points (Figure 3a).

The carbon-flux behavior of a mixotrophic system in any given environmental state (i.e., combination of temperature and nutrients) depends on the arrangement of these equilibria (Figure 3a). A static carbon sink state can occur within a region of low temperatures and high nutrient concentrations, where either a single, stable point equilibrium exists (at low mixotroph density) or a stable point in the lower plane is accompanied by a limit cycle in the upper plane that cannot sustain cycling (Figure 3a, green). Conversely, a static carbon source state occurs when temperatures are higher and nutrient concentrations are lower, associated with either a single, stable, high-mixotroph-density equilibrium point or a stable point in the upper plane that is accompanied by a limit cycle in the lower plane (Figure 3a, red). Interestingly, stationary cycling can occur under any combination of equilibrium points, producing fluctuations in carbon flux between carbon sink and source states (Figure 3a, gray). In some cases, stationary cycling can occur around fixed, stable points, even without limit cycle present (see Discussion section for more information). At high temperatures and nutrient concentrations, hysteresis can occur at temperatures for which both static, stable carbon sink and source states occur (Figure 3a, purple).

Early warning signals for transitions between carbon flux states

Interestingly, increasing nutrient loads erases early warning signals of a shift between carbon sink to carbon source states with warming (Figure 3c–e). Early warning signals come in the form of stationary fluctuations between carbon sink and source states that precede the transition to a static carbon source state as temperature increases (gray region in Figure 3a). Indeed, at low nutrient concentrations ($N_M = 0.6 \text{ ng L}^{-1}$), increasing temperatures produces a large temperature window over which stationary cycling and fluctuations in carbon flux dynamics occur before the system eventually locks in to a static carbon source state (Figure 3e). As nutrient concentration

increases, the range of temperatures that produce fluctuations shrinks (gray region in Figure 3a) and alternative stable point equilibria begin to overlap at intermediate temperatures (Figure 3d). When nutrient concentrations become high enough, stationary cycles completely disappear and alternative, static point equilibria overlap across a wide range of temperatures (Figure 3a&c). In this case, the warming-induced tipping point to a static carbon source state is abrupt and occurs without warning. Additionally, once warming has shifted the system to a carbon source state, a significant reduction in temperature ($>1^{\circ}\text{C}$) would be required to revert the system back to the carbon sink state (hysteresis; Figure 3c).

Generally speaking, although warming always leads to a transition from a carbon sink state to a carbon source state, whether this transition is preceded by a period of fluctuating carbon flux dynamics (early warning signal) depends on nutrient concentrations. Moreover, increasing nutrients reduces the temperature range over which fluctuating carbon flux dynamics occur (shortening early warning signals) while also increasing the temperature range over which static carbon sink and source states overlap (widening hysteresis) (Figures 3a & 4).

DISCUSSION

Mixotrophic organisms and their prey can be considered a unique type of food web module that dynamically transitions between autotrophy (single-species or competitive dynamics) and heterotrophy (consumer-resource dynamics), generating surprising dynamical behaviors that can have important—albeit largely unknown—impacts on ecosystem functioning in novel environments. Here we show how warming can shift mixotrophic systems from a photosynthesis-dominant net carbon sink (Figure 2a&e), through alternative stable carbon states

(Figure 2b&f), and ultimately to a predation-dominant net carbon source (Figure 2c&g). These transitions are preceded by early warning signals in the form of fluctuations between carbon source and sink states when nutrient concentrations are low (Figure 3a&e). But increasing nutrient levels erases these early warning signals by replacing cyclic behavior with alternative, static carbon sink and source states (hysteresis; Figure 3a&c). Taken together, this suggests that mixotrophic systems will tend to shift from carbon sinks to carbon sources with warming and this transition will be more abrupt and less reversible when combined with increased nutrient levels. Given the ubiquity of mixotrophs across all types of ecosystems (Sanders 1991; Stoecker 1998; Mieczan 2009; Worden *et al.* 2015; Selosse *et al.* 2017; Stoecker *et al.* 2017; Flynn *et al.* 2019), our results uncover a potentially crucial but previously unknown aspect of ecosystem responses to global change.

Ecologists have been concerned about identifying how changing environmental conditions might produce tipping points and abrupt regime shifts for decades (Holling 1973; May 1977; Scheffer *et al.* 2001; Folke *et al.* 2004; Dakos & Hastings 2013; Dakos *et al.* 2019). Our study exposes a new mechanism by which abrupt regime shifts may occur—through the unique dynamics of mixotrophic organisms. We find that early warning signals of such shifts may occur in the form of fluctuating dynamics that bridge a transition between static carbon sink and carbon source states. However, we also find that these early warning signals may be environmentally context-dependent—the nature of regime shifts across one environmental gradient might depend on the state of separate environmental factors (as is also evident in some empirical examples of regime shifts (Folke *et al.* 2004)). In our system, the window of early warning signals with warming (e.g., fluctuations spanning temperature changes of $\sim 0.25^{\circ}\text{C}$ vs $\sim 1.5^{\circ}\text{C}$ in Figures 2d and 2e,

respectively), and indeed their very existence (e.g., the lack of fluctuations in Figure 2c), depends on coordinated changes along multivariate environmental gradients (temperature and nutrient concentrations in our case). This finding that specific, multivariate environmental contexts control the nature of regime shifts could also shed light on why tipping points are so elusive in nature (Connell & Sousa 1983; Dudley & Suding 2020; Hillebrand *et al.* 2020). We propose that mixotrophs are not only integral to ecosystem responses to climate change (Jassey *et al.* 2015), but also provide an early warning for carbon tipping points and an opportunity to study complex regime shifts and variation in early warning signals across multivariate environmental gradients.

There is growing recognition that temperature and nutrients interact to impact the structure and dynamics of ecological communities (Binzer *et al.* 2012, 2016; Gilbert *et al.* 2014; Sentis *et al.* 2014; Han *et al.* 2022). Discovering conditions under which temperature-nutrient interactions occur and which properties of ecological systems are affected (e.g., species extinction risk, food web structure and stability, etc.) is of particular interest. Our results show that increasing temperature leads to important dynamical shifts across alternative stable states in mixotrophic systems, but whether this change involves stationary cycling (fluctuating alternative stable states) or hysteresis (static alternative stable states) is controlled by nutrients (Figures 3 & 4). As a result, nutrient levels mediate the impacts of warming on carbon flux dynamics and also determine our ability to predict abrupt transitions between alternative carbon flux states. The critical condition producing this previously unrecognized temperature-nutrient interaction in our model is the dynamic balancing of carbon uptake (via photosynthesis) and carbon release (via respiration) due to flexible energy acquisition strategies in mixotrophs. However, it is possible

that the temperature-nutrient interaction studied here might extend beyond mixotrophic systems to other multispecies systems that also dynamically balances carbon uptake and carbon release (i.e., systems that include both autotrophs and heterotrophs). Determining the generality of this type of temperature-nutrient interaction is an interesting question and area for future research.

The mixotrophic system studied here produces some highly unusual behaviors that have rarely—if ever—been described in ecological systems. Specifically, our model produces a strange and unique form of tri-stability—two alternative stable foci and stable cycling around these points (Figures 2b & 3d)—with important associated impacts on carbon flux dynamics. Another example of unusual behavior occurs when nutrient concentration is low (Figure 3e): some temperatures (19.24–19.65°C) produce stationary cycling around a single fixed-point equilibrium (i.e., a single stable focus that is encircled by two limit cycles—one outer, stable cycle and one inner, unstable cycle). In this situation, the system can produce two possible long-term behaviors: i) dampened oscillations toward the stable focus point when initial conditions are inside the inner, unstable limit cycle or ii) stationary cycling around this stable point when initial conditions are outside the unstable limit cycle. This specific arrangement of coexisting attractors has been observed before in non-ecological systems (De Carvalho Braga & Mello 2013), but to our knowledge, it has yet to be described in an ecological system. The dynamics in each of these examples are a direct result of the flexible carbon acquisition strategies of mixotrophs and variation in environmental conditions, suggesting that other unusual dynamics are possible, or even common, in mixotrophic systems and probably vary across environments. Hence, investigating the dynamical behaviors of mixotrophic systems could fundamentally change our

understanding about the dynamics and structure of microbial communities as well as ecosystem responses to global change.

Our study focuses on a specific type of mixotrophic organism—a primarily predatory organism that uses photosynthesis to supplement energy needs when prey densities are low. But several different types of mixotrophic organisms exist, exhibiting a wide range of mixotrophic strategies and responses to changes in light, nutrient concentrations, and prey densities (Jones 1997; Stoecker 1998; Mitra *et al.* 2016). Each type of mixotroph is likely to produce unique dynamical responses to changes in environmental conditions with different associated impacts on carbon flux. As such, mixotrophs may cause a rich array of novel dynamics that have yet to be uncovered either theoretically or empirically. Although our analysis is based on one specific type of mixotroph, we designed our modeling framework so that it can easily be extended to incorporate the specific resource dependencies of any type of mixotroph simply by defining functional responses for light availability, nutrient concentrations, and prey densities as desired (see Supporting Information for details). In addition, our analysis makes several other assumptions regarding the particular sort of mixotrophic system studied here: two-species system, heterotrophic prey, static nutrient concentrations, single limiting nutrient, fixed stoichiometry, static environments, etc. For example, our analysis considered static nutrient concentrations, but we find that our results are robust to the inclusion of nutrient dynamics (Figure S2). In addition, we focused only on the effects of variation in nutrients utilized by the mixotroph species, however, increasing prey nutrients may mitigate, or even reverse, the transitions between carbon flux states with warming (Figure S3). Furthermore, it remains unclear how explicit competition for resources between a mixotroph and its prey might impact carbon

flux. Relaxing these assumptions could have myriad consequences for dynamics that should be explored in future studies.

Overall, we show that these globally distributed (Sanders 1991; Stoecker 1998; Mieczan 2009; Esteban *et al.* 2010; Worden *et al.* 2015; Selosse *et al.* 2017; Stoecker *et al.* 2017; Flynn *et al.* 2019) and massively abundant (Bar-On *et al.* 2018) mixotrophic microbes exhibit a rich array of dynamical responses to joint changes in temperature and nutrient levels, leading to fundamentally important tipping points between carbon flux states. We also show that nutrient levels determine whether these carbon tipping points are abrupt or accompanied by early warning signals, which is of paramount importance in a rapidly warming and increasingly human-influenced world.

ACKNOWLEDGEMENTS

DJW and JPG, were supported by a U.S. Department of Energy, Office of Science, Office of Biological and Environmental Research, Genomic Science Program Grant award to JPG, under Award Number DE-SC0020362. This work was supported by a grant from the Simons Foundation (Award Number 689265) and NSF Award OCE-1851194 to HVM.

REFERENCES

- Allen, A.P., Gillooly, J.F. & Brown, J.H. (2005). Linking the global carbon cycle to individual metabolism. *Funct. Ecol.*, 19, 202–213.
- Bar-On, Y.M., Phillips, R. & Milo, R. (2018). The biomass distribution on Earth. *Proc. Natl. Acad. Sci. U. S. A.*, 115, 6506–6511.
- Bengtsson, J., Setälä, H. & Zheng, D.W. (1996). Food Webs and Nutrient Cycling in Soils: Interactions and Positive Feedbacks. In: *Food Webs: Integration of Patterns & Dynamics* (eds. Polis, G.A. & Winemiller, K.O.). Springer US, Boston, MA, pp. 30–38.

447 Binzer, A., Guill, C., Brose, U. & Rall, B.C. (2012). The dynamics of food chains under climate
 448 change and nutrient enrichment. *Philos. Trans. R. Soc. B Biol. Sci.*, 367, 2935–2944.
 449 Binzer, A., Guill, C., Rall, B.C. & Brose, U. (2016). Interactive effects of warming, eutrophication
 450 and size structure: impacts on biodiversity and food-web structure. *Glob. Change Biol.*,
 451 22, 220–227.
 452 Bradford, M.A., McCulley, R.L., Crowther, T.W., Oldfield, E.E., Wood, S.A. & Fierer, N. (2019).
 453 Cross-biome patterns in soil microbial respiration predictable from evolutionary theory
 454 on thermal adaptation. *Nat. Ecol. Evol.*, 3, 223–231.
 455 Brown, J.H., Gillooly, J.F., Allen, A.P., Savage, V.M. & West, G.B. (2004). Toward a Metabolic
 456 Theory of Ecology. *Ecology*, 85, 1771–1789.
 457 Connell, J.H. & Sousa, W.P. (1983). On the Evidence Needed to Judge Ecological Stability or
 458 Persistence. *Am. Nat.*, 121, 789–824.
 459 Dakos, V. & Hastings, A. (2013). Editorial: special issue on regime shifts and tipping points in
 460 ecology. *Theor. Ecol.*, 6, 253–254.
 461 Dakos, V., Matthews, B., Hendry, A.P., Levine, J., Loeuille, N., Norberg, J., *et al.* (2019).
 462 Ecosystem tipping points in an evolving world. *Nat. Ecol. Evol.*, 3, 355–362.
 463 De Carvalho Braga, D. & Mello, L.F. (2013). A study of the coexistence of three types of
 464 attractors in an autonomous system. *Int. J. Bifurc. Chaos*, 23, 1350203.
 465 Dell, A.I., Pawar, S. & Savage, V.M. (2011). Systematic variation in the temperature dependence
 466 of physiological and ecological traits. *Proc. Natl. Acad. Sci. U. S. A.*, 108, 10591–10596.
 467 Dell, A.I., Pawar, S. & Savage, V.M. (2014). Temperature dependence of trophic interactions are
 468 driven by asymmetry of species responses and foraging strategy. *J. Anim. Ecol.*, 83, 70–
 469 84.
 470 Dudley, J. & Suding, K.N. (2020). The elusive search for tipping points. *Nat. Ecol. Evol.*, 4, 1449–
 471 1450.
 472 Esteban, G.F., Fenchel, T. & Finlay, B.J. (2010). Mixotrophy in Ciliates. *Protist*, 161, 621–641.
 473 Flynn, K.J., Mitra, A., Anestis, K., Anschütz, A.A., Calbet, A., Ferreira, G.D., *et al.* (2019).
 474 Mixotrophic protists and a new paradigm for marine ecology: where does plankton
 475 research go now? *J. Plankton Res.*, 41, 375–391.
 476 Folke, C., Carpenter, S., Walker, B., Scheffer, M., Elmqvist, T., Gunderson, L., *et al.* (2004).
 477 Regime Shifts, Resilience, and Biodiversity in Ecosystem Management. *Annu. Rev. Ecol.*
 478 *Evol. Syst.*, 35, 557–581.
 479 Gao, Z., Karlsson, I., Geisen, S., Kowalchuk, G. & Jousset, A. (2019). Protists: Puppet Masters of
 480 the Rhizosphere Microbiome. *Trends Plant Sci.*, 24, 165–176.
 481 Geisen, S., Hu, S., dela Cruz, T.E.E. & Veen, G.F. (Ciska). (2021). Protists as catalyzers of
 482 microbial litter breakdown and carbon cycling at different temperature regimes. *ISME J.*,
 483 15, 618–621.
 484 Geisen, S., Lara, E., Mitchell, E.A.D., Völcker, E. & Krashevskaya, V. (2020). Soil protist life matters!
 485 *SOIL Org.*, 92, 189–196.
 486 Gilbert, B., Tunney, T.D., McCann, K.S., DeLong, J.P., Vasseur, D.A., Savage, V., *et al.* (2014). A
 487 bioenergetic framework for the temperature dependence of trophic interactions. *Ecol.*
 488 *Lett.*, 17, 902–914.

489 Graham, E.R., Fay, S.A., Davey, A. & Sanders, R.W. (2013). Intracapsular algae provide fixed
 490 carbon to developing embryos of the salamander *Ambystoma maculatum*. *J. Exp. Biol.*,
 491 216, 452–459.

492 Han, Z.-Y., Wieczynski, D.J., Yammine, A. & Gibert, J.P. (2022). Temperature and nutrients drive
 493 eco-phenotypic dynamics in a microbial food web.

494 Hillebrand, H., Donohue, I., Harpole, W.S., Hodapp, D., Kucera, M., Lewandowska, A.M., *et al.*
 495 (2020). Thresholds for ecological responses to global change do not emerge from
 496 empirical data. *Nat. Ecol. Evol.*, 4, 1502–1509.

497 Holling, C.S. (1973). Resilience and Stability of Ecological Systems. *Annu. Rev. Ecol. Syst.*, 4, 1–
 498 23.

499 Jassey, V.E.J., Signarbieux, C., Hättenschwiler, S., Bragazza, L., Buttler, A., Delarue, F., *et al.*
 500 (2015). An unexpected role for mixotrophs in the response of peatland carbon cycling to
 501 climate warming. *Sci. Rep.*, 5, 16931.

502 Johnson, M.D. & Moeller, H.V. (2018). Editorial: Mixotrophy in Protists: From Model Systems to
 503 Mathematical Models. *Front. Mar. Sci.*, 5, 490.

504 Jones, H. (1997). A classification of mixotrophic protists based on their behaviour. *Freshw. Biol.*,
 505 37, 35–43.

506 Jones, R.I. (2000). Mixotrophy in planktonic protists: an overview. *Freshw. Biol.*, 45, 219–226.

507 Jost, C., Lawrence, C.A., Campolongo, F., van de Bund, W., Hill, S. & DeAngelis, D.L. (2004). The
 508 effects of mixotrophy on the stability and dynamics of a simple planktonic food web
 509 model. *Theor. Popul. Biol.*, 66, 37–51.

510 Kayranli, B., Scholz, M., Mustafa, A. & Hedmark, Å. (2010). Carbon Storage and Fluxes within
 511 Freshwater Wetlands: a Critical Review. *Wetlands*, 30, 111–124.

512 Kuppardt-Kirmse, A. & Chatzinotas, A. (2020). Intraguild Predation: Predatory Networks at the
 513 Microbial Scale. In: *The Ecology of Predation at the Microscale* (eds. Jurkevitch, E. &
 514 Mitchell, R.J.). Springer International Publishing, Cham, pp. 65–87.

515 López-Urrutia, Á., San Martín, E., Harris, R.P. & Irigoien, X. (2006). Scaling the metabolic balance
 516 of the oceans. *Proc. Natl. Acad. Sci.*, 103, 8739–8744.

517 May, R.M. (1977). Thresholds and breakpoints in ecosystems with a multiplicity of stable states.
 518 *Nature*, 269, 471–477.

519 Mieczan, T. (2009). Ciliates in Sphagnum peatlands: vertical micro-distribution, and
 520 relationships of species assemblages with environmental parameters. *Zool. Stud.*, 48,
 521 33–48.

522 Mitra, A., Flynn, K.J., Burkholder, J.M., Berge, T., Calbet, A., Raven, J.A., *et al.* (2014). The role of
 523 mixotrophic protists in the biological carbon pump. *Biogeosciences*, 11, 995–1005.

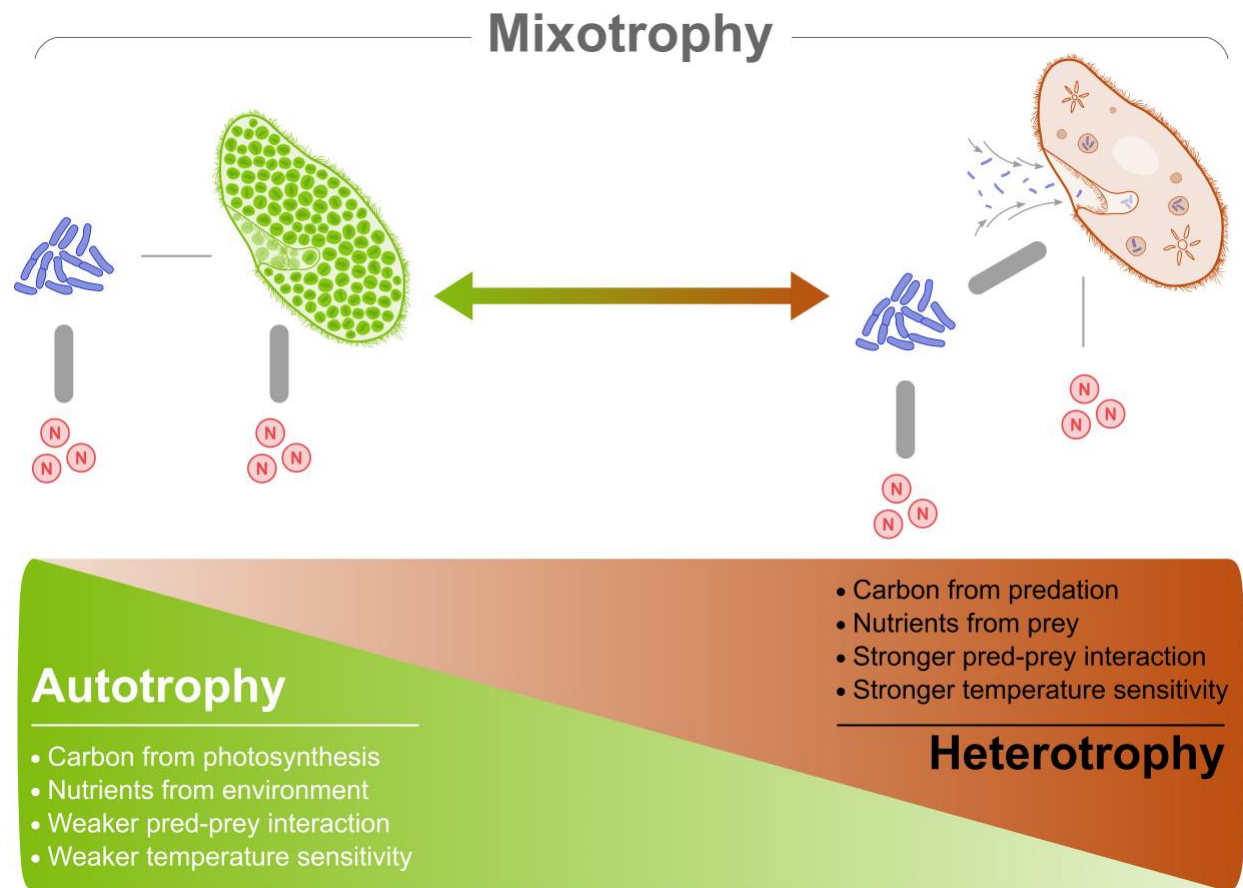
524 Mitra, A., Flynn, K.J., Tillmann, U., Raven, J.A., Caron, D., Stoecker, D.K., *et al.* (2016). Defining
 525 Planktonic Protist Functional Groups on Mechanisms for Energy and Nutrient
 526 Acquisition: Incorporation of Diverse Mixotrophic Strategies. *Protist*, 167, 106–120.

527 Moeller, H.V., Neubert, M.G. & Johnson, M.D. (2019). Intraguild predation enables coexistence
 528 of competing phytoplankton in a well-mixed water column. *Ecology*, 100, e02874.

529 Moeller, H.V., Peltomaa, E., Johnson, M.D. & Neubert, M.G. (2016). Acquired phototrophy
 530 stabilises coexistence and shapes intrinsic dynamics of an intraguild predator and its
 531 prey. *Ecol. Lett.*, 19, 393–402.

532 Moroz, I.M., Cropp, R. & Norbury, J. (2019). Mixotrophs: Dynamic disrupters of plankton
 533 systems? *J. Sea Res.*, 147, 37–45.
 534 Orr, H. (1888). Memoirs: Note on the Development of Amphibians, chiefly concerning the
 535 Central Nervous System; with Additional Observations on the Hypophysis, Mouth, and
 536 the Appendages and Skeleton of the Head. *J. Cell Sci.*, s2-29, 295–324.
 537 Petchey, O.L., McPhearson, P.T., Casey, T.M. & Morin, P.J. (1999). Environmental warming
 538 alters food-web structure and ecosystem function. *Nature*, 402, 69–72.
 539 Rocca, J.D., Yamine, A., Simonin, M. & Gibert, J.P. (2022). Protist Predation Influences the
 540 Temperature Response of Bacterial Communities. *Front. Microbiol.*, 13.
 541 Sanders, R.W. (1991). Mixotrophic Protists In Marine and Freshwater Ecosystems. *J. Protozool.*,
 542 38, 76–81.
 543 Savage, V.M., Gilloly, J.F., Brown, J.H. & Charnov, E.L. (2004). Effects of body size and
 544 temperature on population growth. *Am. Nat.*, 163, 429–441.
 545 Scheffer, M., Carpenter, S., Foley, J.A., Folke, C. & Walker, B. (2001). Catastrophic shifts in
 546 ecosystems. *Nature*, 413, 591–596.
 547 Schimel, J. & Schaeffer, S. (2012). Microbial control over carbon cycling in soil. *Front. Microbiol.*,
 548 3.
 549 Schmidt, S., Raven, J.A., Paungfoo-Lonhienne, C., Schmidt, S., Raven, J.A. & Paungfoo-
 550 Lonhienne, C. (2013). The mixotrophic nature of photosynthetic plants. *Funct. Plant*
 551 *Biol.*, 40, 425–438.
 552 Selosse, M.-A., Charpin, M. & Not, F. (2017). Mixotrophy everywhere on land and in water: the
 553 grand écart hypothesis. *Ecol. Lett.*, 20, 246–263.
 554 Selosse, M.-A. & Roy, M. (2009). Green plants that feed on fungi: facts and questions about
 555 mixotrophy. *Trends Plant Sci.*, 14, 64–70.
 556 Sentis, A., Hemptinne, J.-L. & Brodeur, J. (2014). Towards a mechanistic understanding of
 557 temperature and enrichment effects on species interaction strength, omnivory and
 558 food-web structure. *Ecol. Lett.*, 17, 785–793.
 559 Smith, T.P., Thomas, T.J.H., García-Carreras, B., Sal, S., Yvon-Durocher, G., Bell, T., *et al.* (2019).
 560 Community-level respiration of prokaryotic microbes may rise with global warming. *Nat.*
 561 *Commun.*, 10, 5124.
 562 Steinberg, D.K. & Landry, M.R. (2017). Zooplankton and the Ocean Carbon Cycle. *Annu. Rev.*
 563 *Mar. Sci.*, 9, 413–444.
 564 Stoecker, D.K. (1998). Conceptual models of mixotrophy in planktonic protists and some
 565 ecological and evolutionary implications. *Eur. J. Protistol.*, 34, 281–290.
 566 Stoecker, D.K., Hansen, P.J., Caron, D.A. & Mitra, A. (2017). Mixotrophy in the Marine Plankton.
 567 *Annu. Rev. Mar. Sci.*, 9, 311–335.
 568 Thakur, M.P. & Geisen, S. (2019). Trophic Regulations of the Soil Microbiome. *Trends Microbiol.*,
 569 27, 771–780.
 570 Thingstad, T.F., Havskum, H., Garde, K. & Riemann, B. (1996). On the Strategy of “Eating Your
 571 Competitor”: A Mathematical Analysis of Algal Mixotrophy. *Ecology*, 77, 2108–2118.
 572 Venn, A.A., Loram, J.E. & Douglas, A.E. (2008). Photosynthetic symbioses in animals. *J. Exp. Bot.*,
 573 59, 1069–1080.

Wieczynski, D.J., Singla, P., Doan, A., Singleton, A., Han, Z.-Y., Votzke, S., *et al.* (2021). Linking species traits and demography to explain complex temperature responses across levels of organization. *Proc. Natl. Acad. Sci.*, 118.
 Wilken, S., Huisman, J., Naus-Wiezer, S. & Donk, E.V. (2013). Mixotrophic organisms become more heterotrophic with rising temperature. *Ecol. Lett.*, 16, 225–233.
 Wilken, S., Soares, M., Urrutia-Cordero, P., Ratcovich, J., Ekvall, M.K., Donk, E.V., *et al.* (2018). Primary producers or consumers? Increasing phytoplankton bacterivory along a gradient of lake warming and browning. *Limnol. Oceanogr.*, 63, S142–S155.
 Wolfram Research, Inc. (2021). Mathematica Version 13.0.0, Champaign, Illinois.
 Worden, A.Z., Follows, M.J., Giovannoni, S.J., Wilken, S., Zimmerman, A.E. & Keeling, P.J. (2015). Rethinking the marine carbon cycle: Factoring in the multifarious lifestyles of microbes. *Science*.
 Yang, Z., Zhang, L., Zhu, X., Wang, J. & Montagnes, D.J.S. (2016). An evidence-based framework for predicting the impact of differing autotroph-heterotroph thermal sensitivities on consumer–prey dynamics. *ISME J.*, 10, 1767–1778.
 Yvon-Durocher, G. & Allen, A.P. (2012). Linking community size structure and ecosystem functioning using metabolic theory. *Philos. Trans. R. Soc. B Biol. Sci.*, 367, 2998–3007.
 Zhang, C., Dang, H., Azam, F., Benner, R., Legendre, L., Passow, U., *et al.* (2018). Evolving paradigms in biological carbon cycling in the ocean. *Natl. Sci. Rev.*, 5, 481–499.
 Zhou, J., Xue, K., Xie, J., Deng, Y., Wu, L., Cheng, X., *et al.* (2012). Microbial mediation of carbon-cycle feedbacks to climate warming. *Nat. Clim. Change*, 2, 106–110.



608

609 **Figure 1.** Mixotrophs move dynamically along a spectrum of energy acquisition modes between
610 autotrophy and heterotrophy according to changes in the environment and three essential
611 resources: nutrients, prey, and light. A mixotrophic protist is shown here with its prey (bacteria;
612 blue) and their respective essential nutrients (N). When autotrophy dominates, carbon is obtained
613 primarily via photosynthesis, nutrients come from the environment, and the mixotroph occupies
614 the same trophic level as its prey. When heterotrophy dominates, carbon and nutrients are
615 obtained primarily via predation and the mixotroph occupies a higher trophic level than its prey.
616 As mixotrophs switch between autotrophy and heterotrophy, the mixotrophic food web module
617 shifts between single-species dynamics (or competition, if the mixotroph shares a resource with
618 its prey) and predator-prey dynamics, respectively. The dynamic nature of the mixotrophic food

619 web module likely impacts the structure and dynamics of food webs as well as the flux of matter
620 and energy in broader ecosystems.

621

622

623

624

625

626

627

628

629

630

631

632

633

634

635

636

637

638

639

640

641

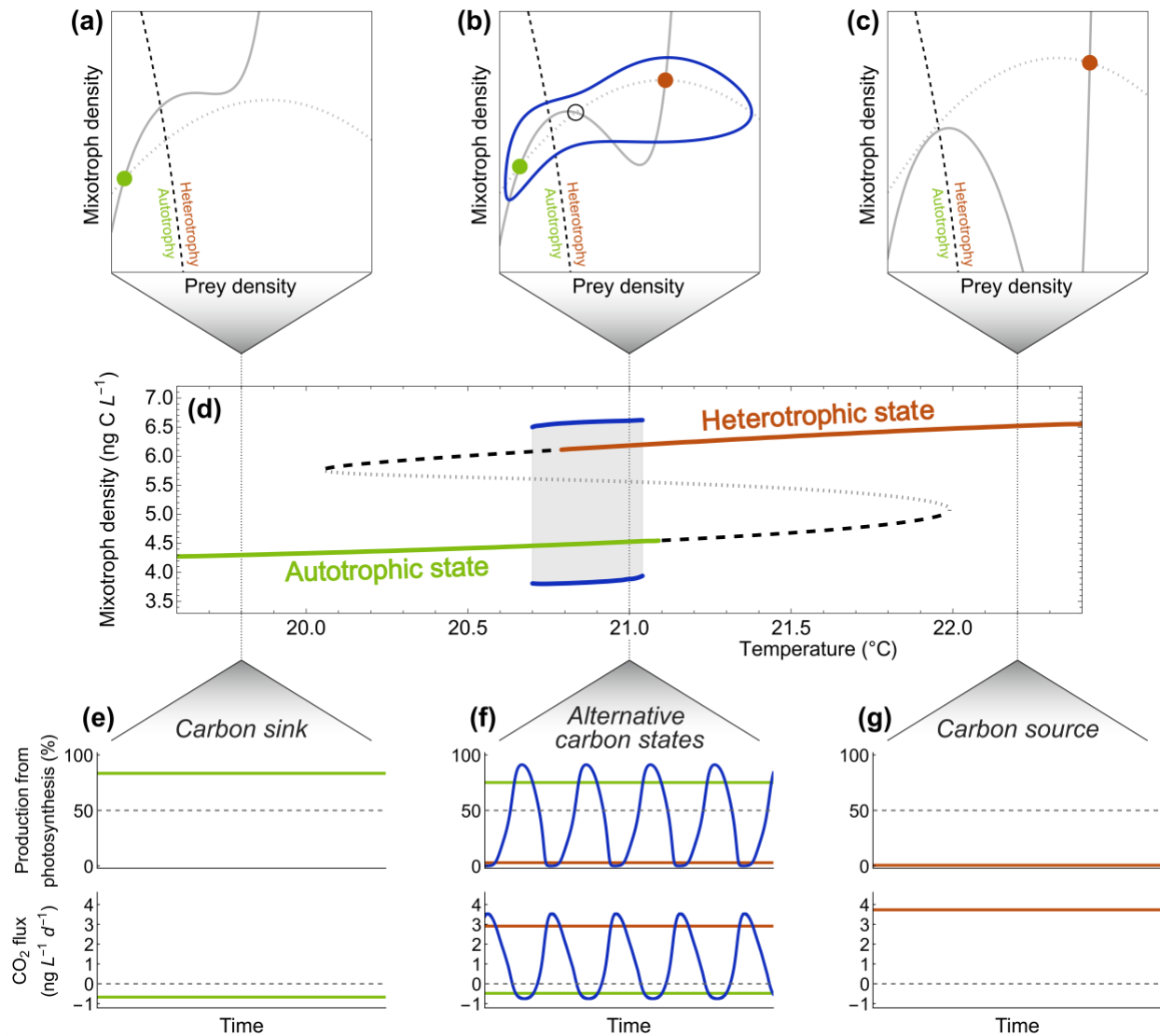


Figure 2. Increasing temperature shifts equilibrium densities, the balance between photosynthesis and consumption, and net CO₂ flux. (a–c) Phase portraits displaying null clines (gray lines) for the prey species (dotted) and the mixotrophic species (solid). Intersections of these null clines represent equilibrium points that are either stable (solid green and red dots) or unstable (open circle). The blue lines indicate stable limit cycles that orbit the three interior equilibria. The black dashed line separates a region where photosynthesis dominates production (left) from a region where predation dominates production (right). (d) A bifurcation diagram displaying transitions between equilibrium scenarios as a function of increasing temperature. (a),

(b), and (c) correspond to temperatures of 19.8°C, 21.0°C, and 22.2°C, respectively. (e–g) Long-term dynamical behavior of the percentage of production from photosynthesis in the mixotroph and the total system net CO₂ flux at 19.8°C, 21.0°C, and 22.2°C, respectively. Colors correspond to stable equilibria and limit cycles in (a–d).

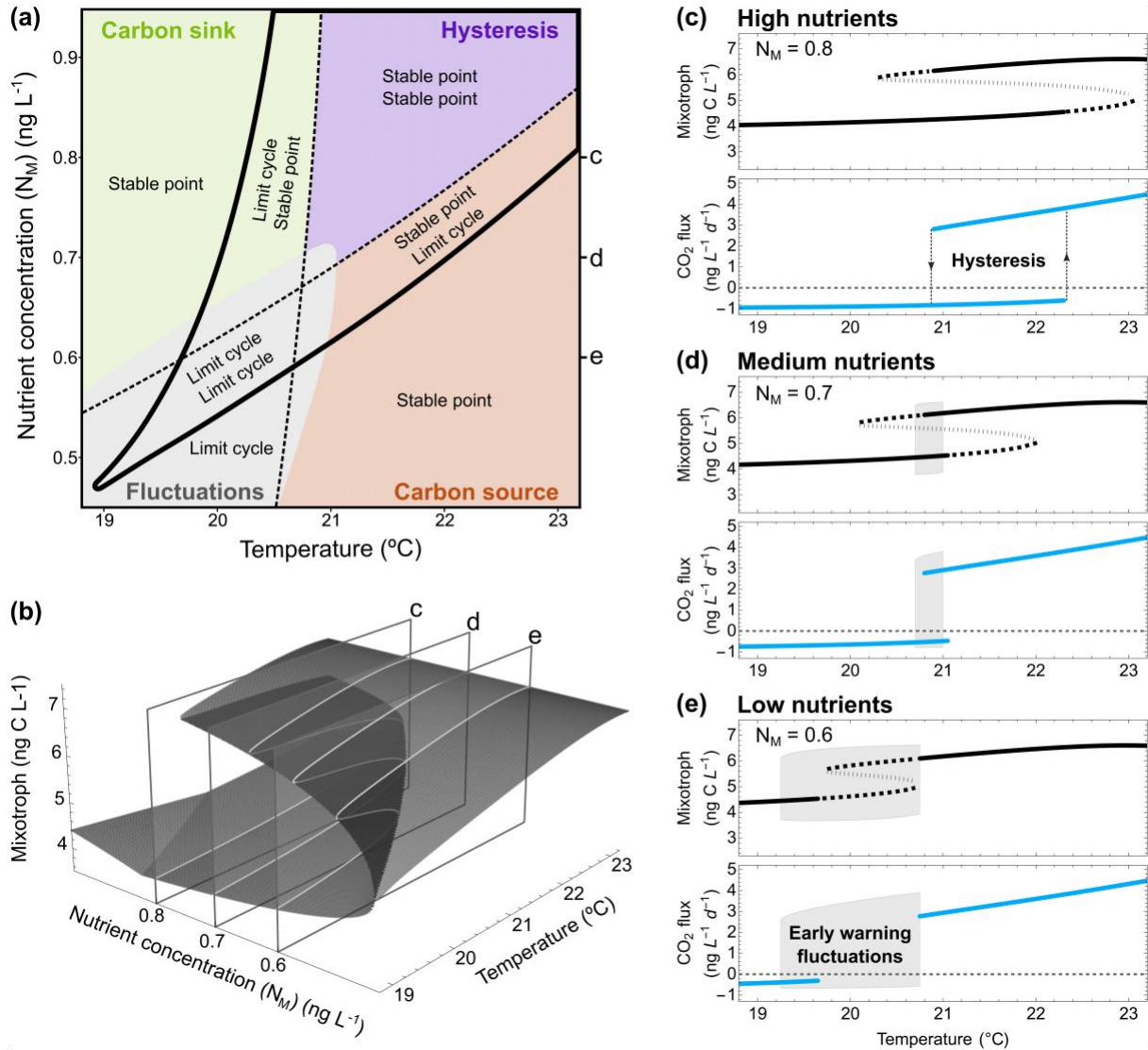


Figure 3. Gradients in temperature and nutrient concentrations produce a rich landscape of equilibrium behaviors. (a) Different environmental conditions produce different equilibrium scenarios with one or two stable points or limit cycles (the solid black line delineates regions with one (outside) or two (inside) equilibria and black dashed lines further subdivide these regions). For regions with two equilibria, the upper and lower text correspond to the orientation of upper and lower equilibria in three-dimensional space (b). The steady-state carbon-flux behaviors of each equilibrium scenario are shown in colored regions: static carbon sink (green), static carbon source (red), fluctuations between carbon sink and source states (gray), and

hysteresis with overlapping carbon sink and source states (purple). (b) In three-dimensional space, equilibria create a folded landscape where the upper and lower planes are either stable points or limit cycles and are separated by an interior plane of unstable equilibria. (c–e) show bifurcation diagrams of equilibrium densities (upper panels) and steady-state CO₂ flux (lower panels) across temperatures for three different nutrient concentrations (indicated by “c”, “d”, and “e” in panels (a) and (b)). Solid lines (black and blue) denote fixed point equilibria, dashed lines denote unstable limit cycle equilibria, gray regions denote stationary cycling (fluctuations), and dotted lines denote unstable equilibria (i.e., the interior plane in (b)).

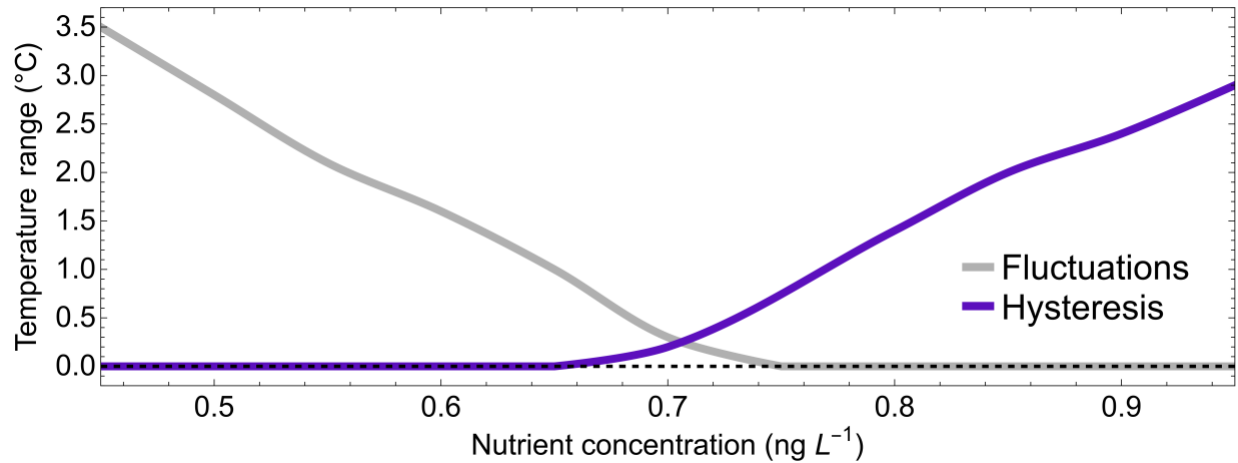


Figure 4. The effect of nutrient concentration on the range of temperatures over which fluctuations in carbon flux (an early warning signal of a carbon tipping point) and overlapping static carbon sink and source states (hysteresis) occur. The decline in fluctuations with increasing nutrients (gray) indicates a reduction in the temperature window producing early warning signals. Increases in the range of temperatures where stable carbon states overlap (purple) indicates increasing hysteresis.

723 **Table 1.** Variables and parameters used in the mixotrophy model.

Variable/Parameter	Definition	Units	Value
M, P	Biomass density	ng C L ⁻¹	na
N_i	Nutrient concentration	ng L ⁻¹	$N_M = [0.4, 1.0]$ $N_P = 0.7$
h_i	Half-saturation constant	ng	$h_M = 0.8$ $h_P = 0.3$
d	Photosynthesis prey dependence decline rate	n/a	0.072
K_i	Carrying capacity	ng C L ⁻¹	$K_M = 10$ $K_P = 19$
ε	Max conversion efficiency	n/a	0.25
Temperature-dependent parameters (following Eqn. 2)			
$\mu_i(T)$	Max production rate	t ⁻¹	$\mu_M(T): b_0 = 0.45; E_a = 0.32$ $\mu_P(T): b_0 = 1.35; E_a = 0.65$
$\alpha(T)$	Attack rate	t ⁻¹	$b_0 = 0.21; E_a = 0.65$
$\delta_i(T)$	Respiration rate	t ⁻¹	$\delta_M(T): b_0 = 0.07; E_a = 0.65$ $\delta_P(T): b_0 = 0.05; E_a = 0.65$
$m_i(T)$	Mortality rate	t ⁻¹	$m_M(T): b_0 = 0.072; E_a = 0.45$ $m_P(T): b_0 = 0.052; E_a = 0.45$

724
725
726
727
728
729
730
731
732
733
734
735

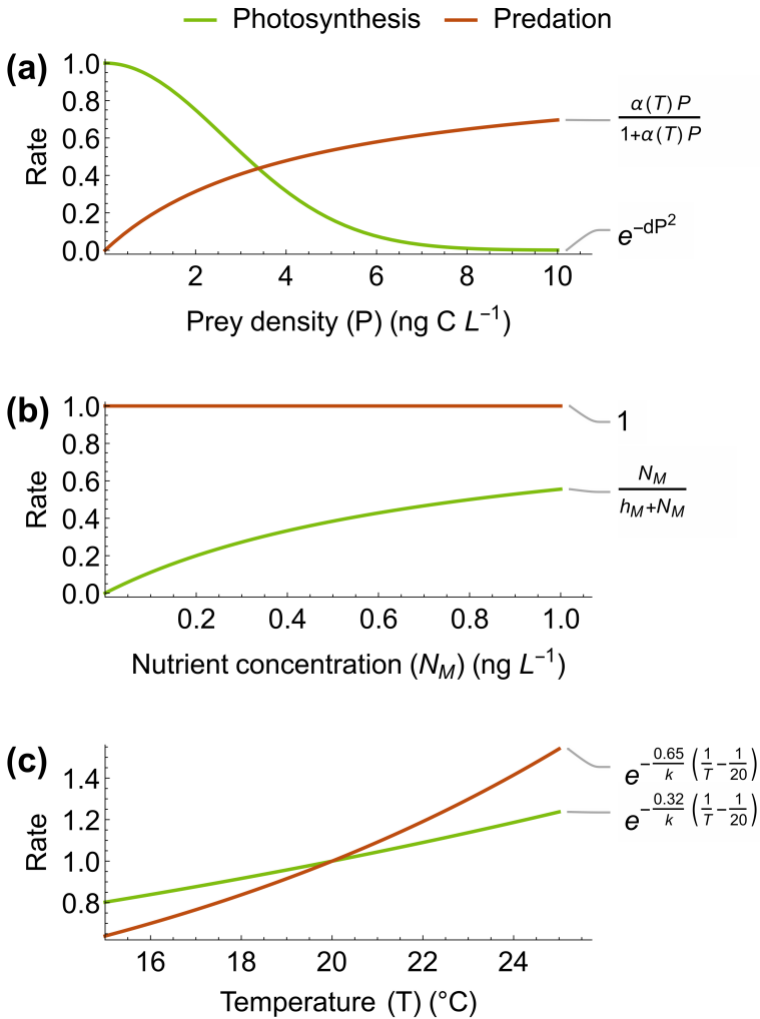


Figure S1. Functional forms of functional responses for mixotroph photosynthesis and predation rates across (a) prey densities, (b) nutrient concentrations, and (c) temperatures.

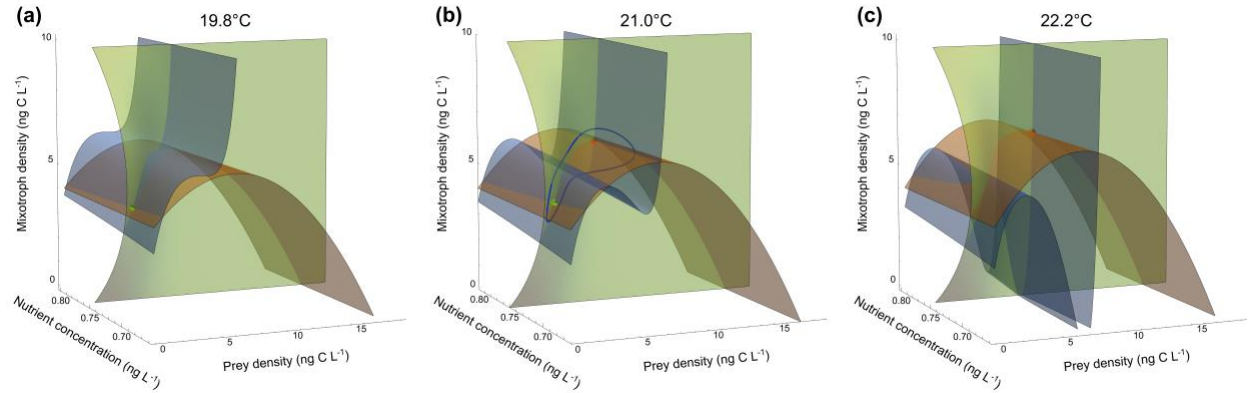


Figure S2. Equilibrium phase space shown for a variation of our mixotrophy model that includes dynamic nutrients for the mixotroph. Orange, blue, and green planes correspond to prey, mixotroph, and nutrient null clines. Intersections of these null clines represent equilibrium points (solid green and red dots) and the blue line indicates stable limit cycles that orbit the interior equilibria (as in Figure 2 in the main text). Although the nutrient dimension introduces more complex equilibria that included changes in nutrient concentrations, the results here are qualitatively the same as in the static nutrient model. In this version of the model, nutrients utilized by the mixotroph follow chemostat dynamics, with reduction due to mixotroph photosynthetic production: $\frac{dN_M}{dt} = \tau(N_{M,feed} - N_M) - M * \varphi(T, N_M, P, M)$, where N_M is the concentration of nutrients utilized by the mixotroph, τ is a dilution rate, $N_{M,feed}$ is a feed concentration for mixotroph nutrients, M is mixotroph density, and φ is the per-capita photosynthetic production rate of the mixotroph. Nutrient model parameters used for the results shown here were $\tau = 10 \text{ ng L}^{-1} \text{ t}^{-1}$ and $N_{M,feed} = 0.75 \text{ ng L}^{-1}$. All other model parameters were the same as used in the main results (Table 1).

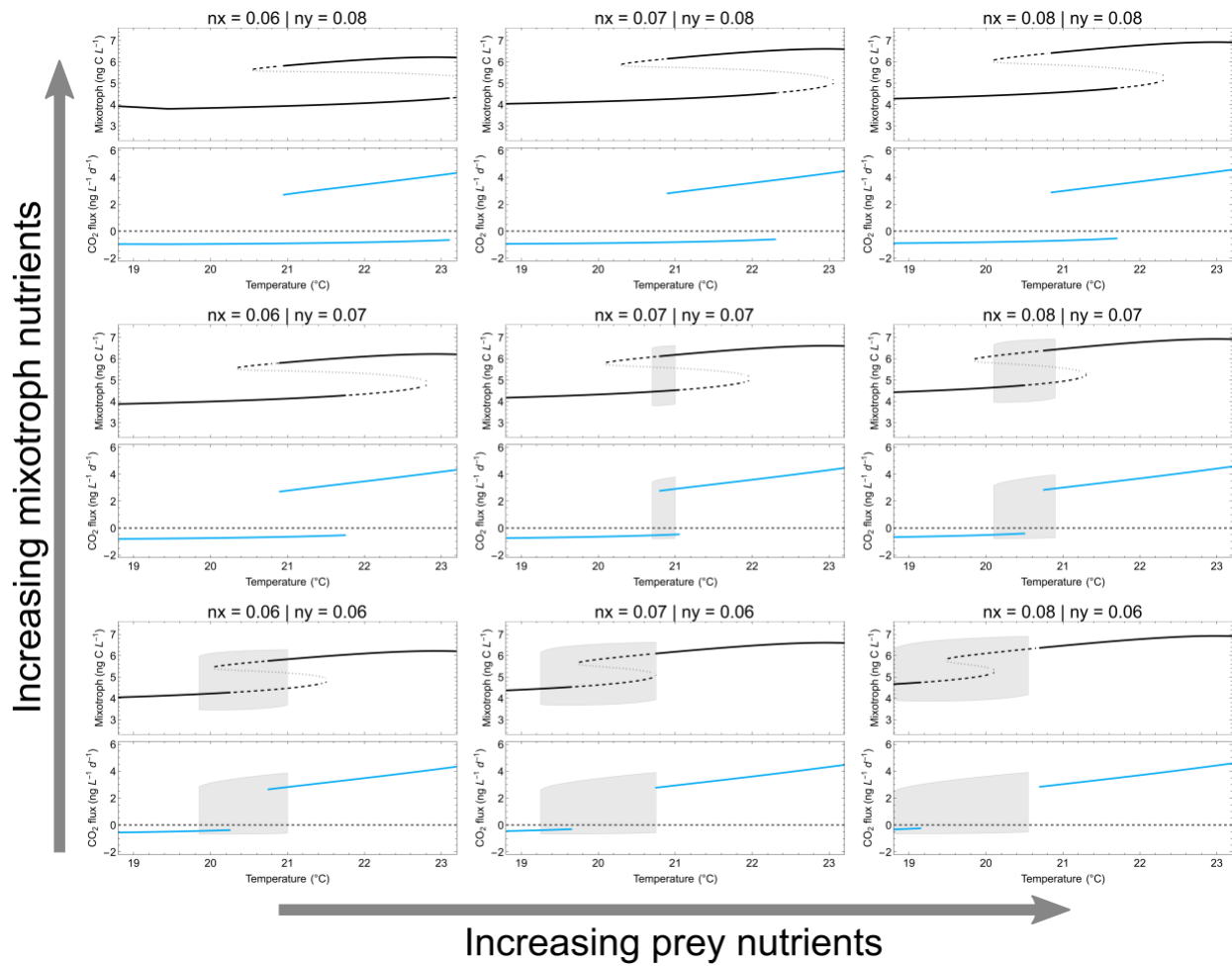


Figure S3. Equilibrium mixotroph densities and net CO₂ flux shown across temperatures and across gradients of nutrient concentrations for nutrients utilized by a mixotroph (vertical) and its prey (horizontal). The center column corresponds to panels c–e in Figure 3 in the main text.